

Osteocyte death during orthodontic tooth movement in mice

Sogole Moin^{a*}; Zana Kalajzic^{b*}; Achint Utreja^c; Jun Nihara^b; Sunil Wadhwa^d; Flavio Uribe^e; Ravindra Nanda^f

ABSTRACT

Objective: To investigate the time course of osteocyte death in a mouse model of orthodontic tooth movement (OTM) and its association to the caspase-3 activation pathway and osteoclast formation.

Materials and Methods: Twenty-five male wild type CD-1 mice (8–12 weeks old) were loaded with an orthodontic appliance. A spring delivering 10–12 g of force was placed between the right first molar and the incisor to displace the first molar mesially. The contralateral unloaded sides served as the control. The animals were equally divided into five different time points: 6, 12, 24, and 72 hours and 7 days of orthodontic loading. Terminal deoxynucleotidyl transferase dUTP nick end labeling (TUNEL) assay, caspase-3 immunostaining, and tartrate-resistant acid phosphatase (TRAP) staining was performed on histologic sections of the first molars. The labeling was quantified in osteocytes on the compression side of the alveolar bone at each time point.

Results: TUNEL labeling significantly increased at 12, 24, and 72 hours after orthodontic loading; the peak was observed at 24 hours. Elevated caspase-3 labeling was noted at 12, 24, and 72 hours and 7 days after loading, although the increase was not significant. Significant osteoclast formation was initially evident after 72 hours and progressively increased up to 7 days.

Conclusions: Osteocyte death during OTM peaks at 24 hours, earlier than initial osteoclast activation. However, only a slight trend for increased caspase-3 activity suggests that other mechanisms might be involved in osteocyte death during OTM. (*Angle Orthod.* 2014;84:1086–1092.)

KEY WORDS: Tooth movement; Osteocyte; Apoptosis

INTRODUCTION

Orthodontic tooth movement (OTM) occurs as a result of alveolar bone remodeling in response to an

applied force that produces two different regions in the periodontal ligament (PDL): compression and tension. On the compressed side, there is a disturbance of blood flow and cell death (hyalinization), followed by resorption of the hyalinized tissue by macrophages. On the tension side, stretched PDL fibers are associated with increased blood flow. Overall, increased osteoclast activity leads to bone resorption in areas of compression, whereas increased osteoblast activity leads to bone formation in areas of tension.¹

Osteocytes, which normally respond to an externally applied force during OTM by changing the expression levels of many genes,^{2–4} may play a significant role in mechanosensing and regulating bone remodeling.^{5,6} Dying osteocytes have been proposed to play a specific role in recruiting osteoclasts to remodeling sites. A study showed that adding osteocyte apoptotic bodies (derived from MLO-Y4 cells) to the murine parietal bone resulted in osteoclast-mediated bone resorption.⁷

The two major types of cell death are apoptosis, or programmed cell death, and necrosis, or accidental cell death. Various methods to distinguish apoptotic and necrotic cells in vitro have been developed and

* The first two authors contributed equally to this work.

^a Private Practice, Clinician, Manchester, NH.

^b Research Fellow, Department of Craniofacial Sciences, University of Connecticut Health Center, Farmington.

^c Resident, Department of Craniofacial Sciences, University of Connecticut Health Center, Farmington.

^d Associate Professor and Chair, Division of Orthodontics, Columbia University College of Dental Medicine, New York, NY.

^e Associate Professor, Department of Craniofacial Sciences, University of Connecticut Health Center, Farmington.

^f Professor and Chair, Department of Craniofacial Sciences, University of Connecticut Health Center, Farmington, CT.

Corresponding author: Dr Zana Kalajzic, Department of Craniofacial Sciences (Division of Orthodontics), L7059, University of Connecticut Health Center, Mail Code 1725, 163 Farmington Ave, Farmington, CT 06030 (e-mail: zkalajzic@uchc.edu)

Accepted: February 2014. Submitted: November 2013.

Published Online: April 2, 2014

© 2014 by The EH Angle Education and Research Foundation, Inc.

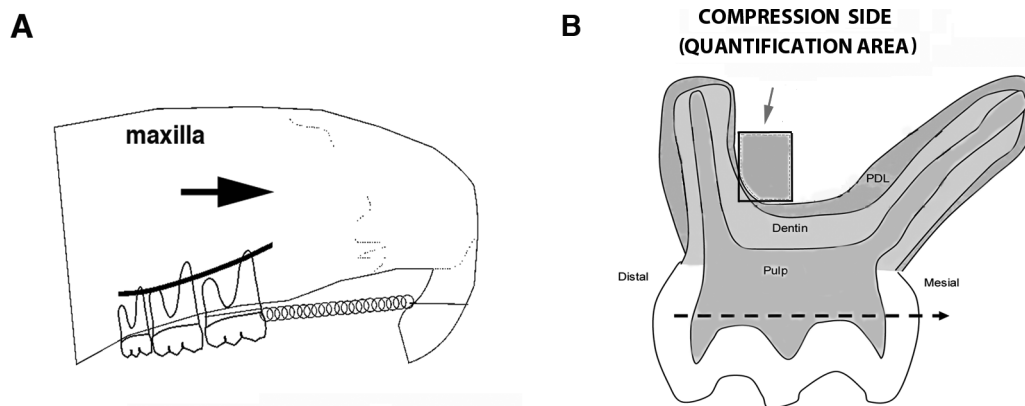


Figure 1. (A) Schematic of mouse OTM model. A spring delivering 10–12 g was activated from the right first maxillary molar to the right incisor. The arrow shows the force direction. (B) Schematic illustration of that quantification area (black box) on the compression side of distobuccal root. The arrow points to alveolar bone (grey) selected for quantifying only apoptotic osteocytes.

validated using electron microscopy and flow cytometry techniques, mostly based on cell morphology and the function of cell organelles, cell viability assays, the ability of DNA to resist endonucleolytic DNA degradation, and typical biochemical cell death features.⁸

It has been reported that the major mechanisms regulating apoptosis in bone,⁹ the extrinsic and intrinsic pathways, merge at the level of the effector caspases such as caspase-3, which is required for the formation of apoptotic bodies, a typical hallmark of apoptosis.¹⁰ Caspase-3 is thus considered a marker of apoptosis in bone studies, and its localization marks the initiation of the apoptotic process.

To date, little is known about the regulation of osteocyte death during OTM. Although some *in vivo* studies^{11,12} report that osteocytes could undergo apoptosis during OTM, their results are based on morphologic changes in nuclei. Biochemical changes in the dying osteocytes, reflected by expression of specific apoptotic markers, have yet to be explored.

This study aimed to investigate the timing of osteocyte death in an *in vivo* mouse model of OTM and to correlate it with the temporal expression of active caspase-3. Although some studies have already examined the time course of osteoclast formation during OTM,¹² we also wanted to explore how the time course of osteocyte death correlates with osteoclast formation in our OTM model.

MATERIALS AND METHODS

Study Design

Experiments were performed under an institutionally approved protocol for the use of animals in research (ACC#100132-0514). In total, 25 CD-1 male mice (8–12 weeks old) were used for the study. Mice were equally divided into five groups: 6, 12, 24, and 72 hours

and 7 days of OTM. An orthodontic spring was placed in all animals between the maxillary right first molar and incisor. Left maxillae were not loaded and served as contralateral controls. The mice were housed under normal laboratory conditions and weighed daily. They were fed powdered food and water *ad libitum*.

Application of Orthodontic Appliance

Orthodontic appliances were placed under general anesthesia according to the protocol described by Olson et al.¹³ (Figure 1A). The force deflection rate of the spring (F/Δ) was determined to be in the range of 10–12 g. The appliances were checked daily to ensure their integrity.

Tissue Preparation for Histologic Analysis

Upon completion of the time course, mice were killed by CO₂. The maxillae were hemisected, dissected, and placed in 10% formalin for 7 days at 4°C. After fixation, maxillae were decalcified in 14% EDTA at 4°C for 5 weeks, processed with a series of ethanol concentrations, and embedded in paraffin. Next, 5- μ m serial sagittal sections were cut using a Leica microtome RM 2125R7 (Leica Microsystems Inc, Buffalo Grove, IL, USA).

TUNEL Assay and Quantification

To detect DNA fragments derived from dead cells, the terminal deoxynucleotidyl transferase dUTP nick end labeling (TUNEL) assay was used. Deparaffinized sections were stained with the DeadEnd Fluorometric TUNEL System (G3250, Promega Corp, Madison, Wis) according to the manufacturer's instructions. The fluorescein-12-dUTP-labeled DNA was visualized by fluorescence microscopy using a Zeiss Axiovert 200 microscope (Carl Zeiss, Thornwood, NY, USA) and

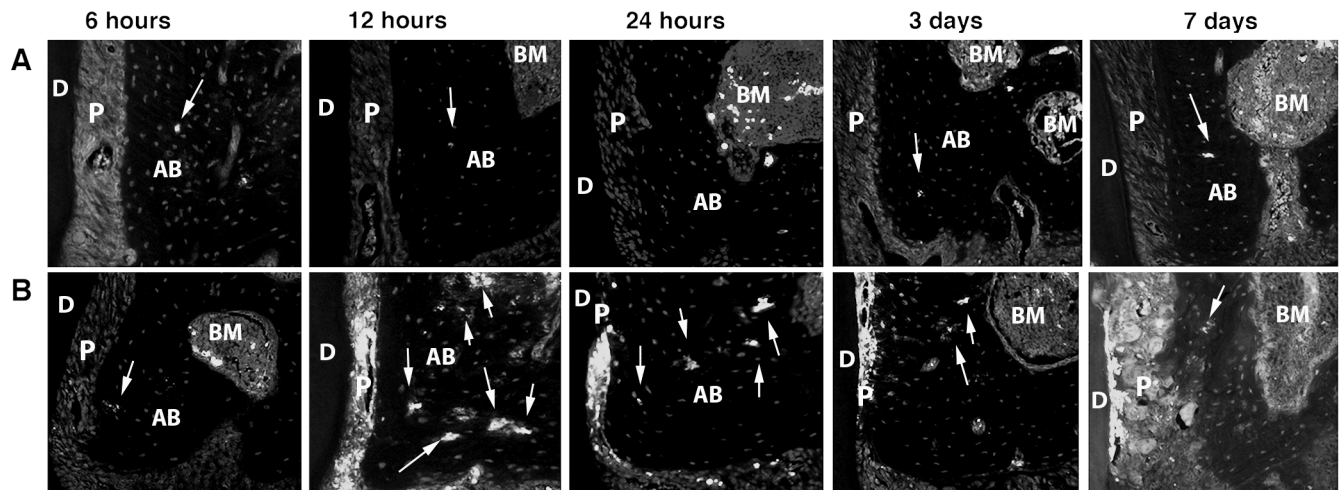


Figure 2. (A,B) Time course of TUNEL labeling on the compression in control (panel A) and loaded maxillae (panel B). The arrows point to TUNEL-positive osteocytes. The highest number of labeled osteocytes was noticed at 12 hours, 24 hours, and 3 days of OTM. D indicates dentin; P, PDL; AB, alveolar bone; BM, bone marrow.

digital camera, and 4',6-diamidino-2-phenylindole (DAPI) staining was performed to quantify total cells (Figure 2A,B).

Three molar sagittal sections revealing the most pulp and dentin structure of the mesiobuccal and distobuccal roots (midroot sections) from each animal were analyzed. For quantification, a rectangular box of fixed area (4×3 inch) was superimposed on 10× images on the compression side of alveolar bone (mesial surface of the distobuccal root) (Figure 1B). TUNEL-positive osteocytes were counted in the defined box and normalized per number of DAPI-positive osteocytes on the overlaid fluorescent images. The ratio of cells was calculated for each section as TUNEL positive osteocytes/total osteocytes. The ratios from three sections were then averaged for each mouse. The values from five different animals at each time point were used to conduct statistical tests.

Immunohistochemistry on Active Caspase-3 and Quantification

Deparaffinized sections were incubated with 0.3% H₂O₂ in phosphate buffered saline for 20 minutes. Heat-mediated antigen retrieval was performed by immersing the slides in 1× citrate buffer (pH 6.0) at 60°C overnight. The next day, sections were washed and blocked with 10% normal goat serum for 2 hours at room temperature and then incubated with primary rabbit polyclonal anti-caspase-3 antibody (ab4051, Abcam, Cambridge, Mass) overnight at +4°C at a concentration of 1:75. After incubation with a goat biotinylated secondary antibody, the signal was developed with a biotin/avidin system. Secondary antibody and developing reagents (DAB; 3,3'-diaminobenzidine tetrahydrochloride) were part of the Vector Elite ABC kit (PK6101, Vector Laboratories,

Burlington, Calif). The sections were counterstained with Harris hematoxylin.

Three sections from four different mice at each time point were analyzed. Similar to TUNEL quantification, a rectangular box of fixed area (4×8 inch) was superimposed on 20× brightfield images on the compression side of the distobuccal root. Caspase-3 positive osteocytes were counted and normalized per total osteocytes in the defined box to get a ratio of positive osteocytes. The ratios from three sections were averaged for each mouse, and those values were used to conduct statistical tests.

TRAP Staining and Osteoclast Quantification

Staining for tartrate-resistant acid phosphatase (TRAP) activity was performed by using an acid phosphatase leukocyte kit (Sigma Chemical, St Louis, Mo) according to the manufacturer's instructions. Midroot molar sections were analyzed, and the area for quantification on the mesial side of the distobuccal root was identified as a square parallel to the sagittal axis of the distobuccal root with one side 150 μm wide and the other extending from the root bifurcation to the apex. Histo-morphometry analyses were carried out using Osteomeasure software (OsteoMetrics, Inc, OsteomeasureTM Version 1.01, Decatur, GA).

Three sections from four different mice, representing the loaded and control sides at each time point, were analyzed. The osteoclast counts were then averaged for each mouse and included in the statistical tests.

Statistical Analysis

Statistical analyses were carried out using GraphPad Prism (GraphPad Software, Inc, Version 5.0a, La Jolla,

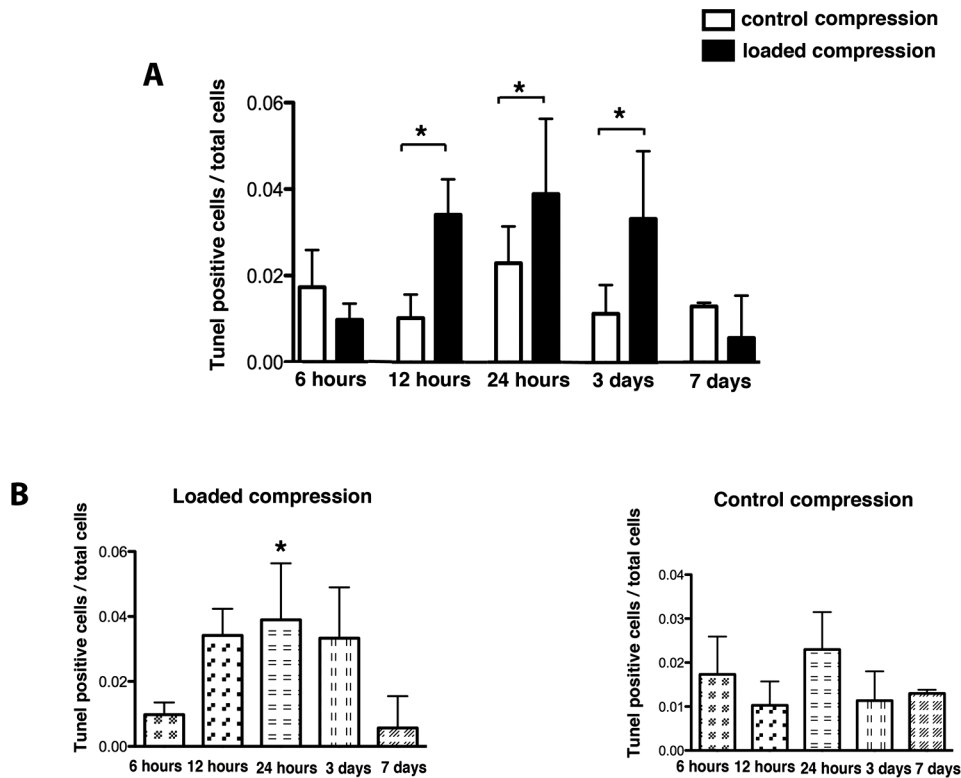


Figure 3. (A) Quantification of TUNEL-positive osteocytes at 6 hours ($P = .114$), 12 hours ($P = .0016$), 24 hours ($P = .0385$), 72 hours ($P = .0203$), and 7 days ($P = .2658$) (unpaired t -test, $n = 5$). (B) Left: a graph showing the peak of TUNEL labeling on the compression 24 hours after loading ($P = .0018$, one-way ANOVA, $n = 5$). Right: No significance was noticed in TUNEL labeling between different time points in control maxillae ($P = .1032$, one-way ANOVA, $n = 5$).

CA, USA). Statistical significance of differences among means was determined by paired or unpaired t -tests and one-way analysis of variance (ANOVA) tests with a Bonferroni post-hoc test. Significance was set at $P < .05$.

RESULTS

Individual unpaired t -tests at each time point revealed a statistically significant increase in TUNEL-positive cells on the loaded compression at 12 hours ($P = .0016$), 24 hours ($P = .0385$), and 72 hours ($P = .0203$). However, at 6 hours and at 7 days, there was no difference between the sides ($P = .1114$, $P = .2658$, respectively), indicating that osteocyte death either stayed the same or returned to normal at those time points (Figure 3A).

Comparing all time points, a statistically significant increase in TUNEL labeling was detected on the loaded compression at 24 hours (one-way ANOVA, $P = .0018$), indicating that the peak of osteocyte death occurred at 24 hours. There was no difference on the control compression, which suggests that osteocyte death occurs only on the loaded compression (one-way ANOVA, $P = .1033$) (Figure 3B).

To detect the changes in caspase-3-positive osteocytes, paired t -tests were used to compare control and loaded compression sides at each time point to avoid

the background differences related to different staining times.

At 12 hours, the number of caspase-3-positive osteocytes was slightly increased but not significantly ($P = .0866$). This trend continued at 24 hours ($P = .9551$) and 72 hours ($P = .2033$) and it was not as pronounced at day 7 ($P = .8357$) (Figure 4B).

To detect the initiation of osteoclast formation, quantification was performed on the mesial side of the distobuccal root from the furcation to the apex. At 6, 12, and 24 hours, there was no noticeable difference in osteoclast number between the control and loaded compression sides ($P = .4629$, $P = .9945$, $P = .2910$, respectively). However, a significant increase in osteoclast formation on the loaded compression was noted on day 3 ($P = .00321$). This increase was more prominent at day 7 ($P = .0107$), suggesting marked bone resorption at that time point (Figure 5).

DISCUSSION

Because recent research suggests that osteocyte apoptosis may induce osteoclast recruitment,¹⁴⁻¹⁶ this study aimed to further investigate osteocyte death in a mouse model of OTM.

Based on the TUNEL assay, our results showed significant osteocyte death at 12 hours, peaking at

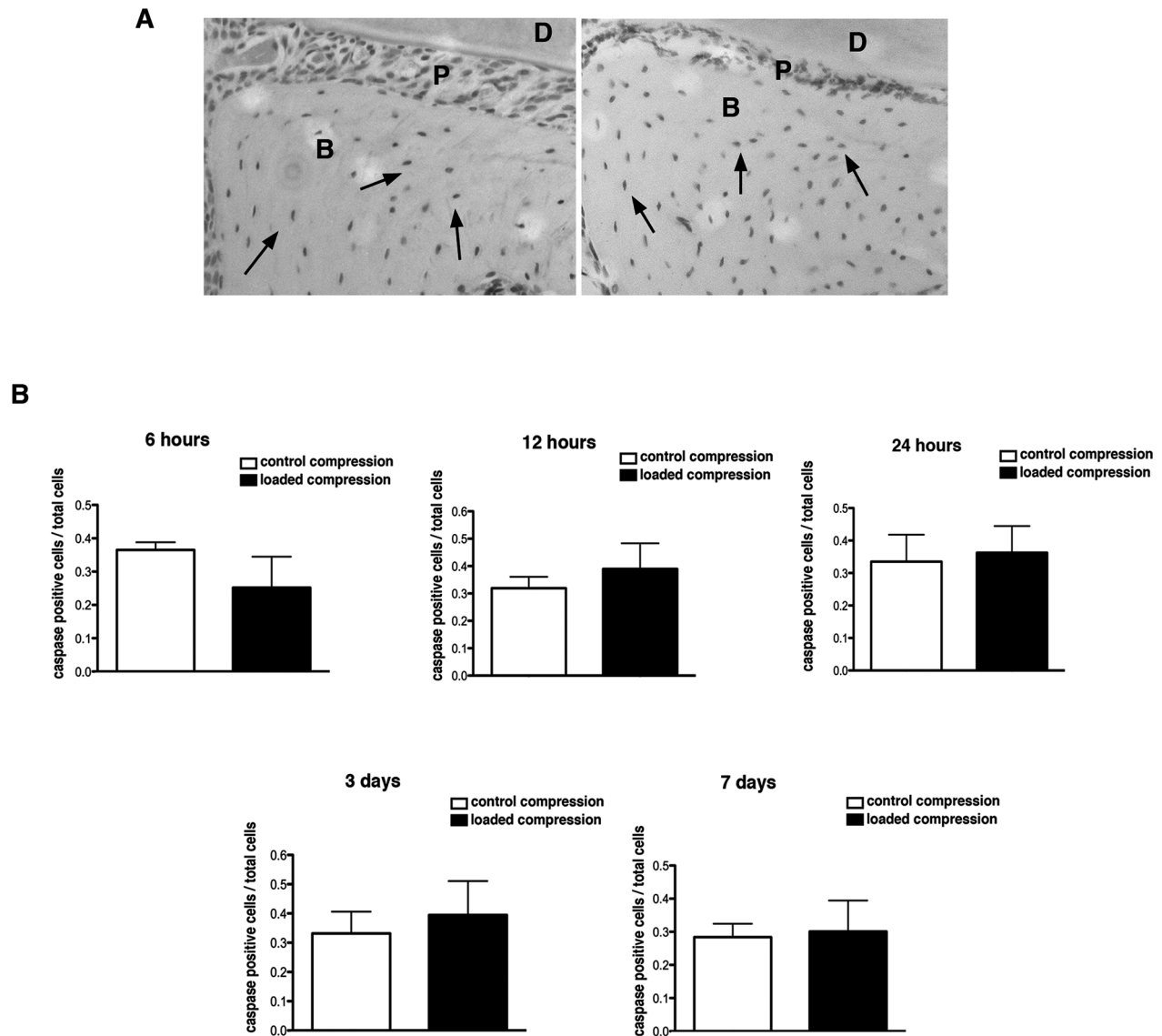


Figure 4. (A) Example of caspase-3 immunostaining on the compression of control and loaded maxillae after 12 hours of OTM. The arrows point to positive osteocytes (20 \times). (B) Quantification of caspase-3-positive osteocytes at 6 hours ($P = .1254$), 12 hours ($P = .0866$), 24 hours ($P = .9551$), 72 hours ($P = .2033$), and 7 days ($P = .8357$) (paired t -test, $n = 4$). Note no significance in any of experimental time points.

24 hours. These levels were still significantly elevated at 72 hours and then returned to the base level at day 7. These findings are similar to the results of Sakai et al.,¹² who found that TUNEL labeling increased progressively with peaks at 12 and 24 hours; however, that study did not delineate the exact mechanism involved because of the nonspecificity of the TUNEL assay.¹⁷ On the other hand, Hamaya et al.¹¹ used a rat OTM model and detected apoptotic changes in osteocytes as early as 6 hours of OTM. In contrast to our study, their observation was based on nuclear morphologic changes, such as nuclear fragmentation and chromatin condensation. They also reported some necrotic processes at later time points.

In this study, we observed caspase-3-labeled osteocytes that increased slightly at 12 hours and

continued to be present throughout the duration of OTM. However, as this change was not significant, it suggests that caspase-3 involvement in osteocyte death during OTM is only partial, and not the predominant underlying mechanism. It has been reported that the TUNEL assay is not specific for labeling apoptotic cells as it also detects some necrotic changes.¹⁷ This raises the possibility that some of the TUNEL-positive osteocytes in our study actually underwent necrosis. It has been shown that in the absence of phagocytosis, apoptotic cells proceed to secondary necrosis.¹⁸ These secondary necrotic cells have already gone through an apoptotic stage and now exhibit many morphologic features of primary necrotic cells. Similar to the findings of Hamaya et al.,¹¹ it is possible that apoptosis starts with the

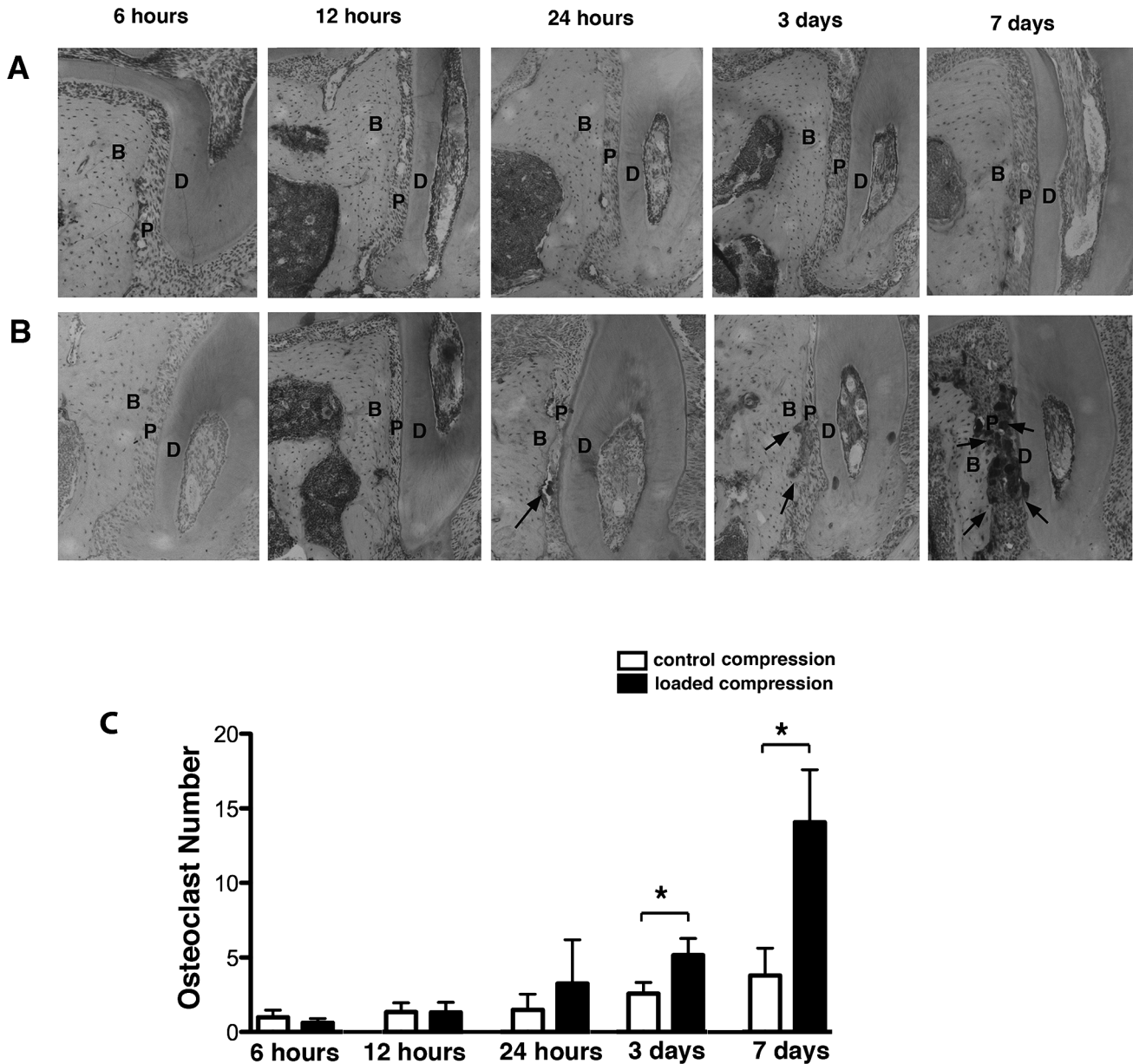


Figure 5. (A,B) TRAP staining in control (panel A) and loaded (panel B) maxillae in different OTM time points on the compression side. Osteoclasts were slightly elevated at 24 and 72 hours of OTM (arrows) and remarkably increased at day 7. (C) Quantification of active osteoclasts (>2 nuclei) at 6 hours ($P = .4629$), 12 hours ($P = .0994$), 24 hours ($P = .2910$), 72 hours ($P = .0032$), and 7 days ($P = .0107$) (paired t -test, $n = 4$). Note the significant increase at 72 hours and 7 days.

activation of caspase-3 but then quickly proceeds to necrosis.

The PDL exhibited a high level of TUNEL activity. We also observed considerable hyalinization of the PDL at 72 hours (not shown), suggesting that the amount of force applied (10–12 g) could have been too great. Hamaya et al.¹¹ applied 10.5 g of force in 8-week-old Wistar rats, which are much larger than mice. Considering this, it could be possible that the involvement of particular pathway (apoptosis versus necrosis) depends on the amount of compressing force applied to the alveolar bone.

Although caspases have been considered the major executors of apoptosis, there is evidence that apoptotic changes can occur even in their absence. The various forms of caspase-independent cell death cannot readily be classified as apoptosis or necrosis, and alternative types of programmed cell death, such as autophagy, paraptosis, and mitotic catastrophe, have been described.¹⁹ Necroptosis, or programmed necrosis, has also been found as an alternative form of cell death^{20,21} where receptor interacting protein-1 (Rip-1) plays a critical role. However, in our preliminary data, no change in the expression of Rip 1 was

observed in alveolar osteocytes during OTM (results not shown).

The increase in osteoclast recruitment was not significant before 72 hours and was particularly evident at day 7. This suggests that osteoclastogenesis commences much later than the peak of osteocyte apoptosis, confirming that osteocyte death is necessary before osteoclast formation. Overall, the importance of osteocyte apoptosis/death in the initiation of bone remodeling during OTM is now highlighted. Interestingly, a slight increase in osteoclast number was detected on the contralateral compression, which could suggest that secretion of factors needed for osteoclast recruitment occurs not only locally but also systemically.

A recent study reported contradictory results where osteocyte death under certain conditions decelerated OTM.²² Other data suggest that RANKL (Receptor activator of nuclear factor kappa B ligand) production, which is necessary to initiate osteoclastogenesis, might be related to osteocytic apoptotic bodies.¹⁵ Therefore, it is possible that osteocytes undergoing different types of death, apoptosis or necrosis, may release different signals to osteoclast precursors.

Although the *in vivo* investigation of apoptosis, particularly nuclear morphology, in fixed tissue is challenging because of the architectural complexity of the tissues and the difficulty of using vital nuclear stains, more studies are needed to delineate the exact mechanism of osteocyte death during OTM. The accurate detection of a specific pathway is not an easy process, and it should be based on the combination and integration of many different techniques used at the same time. A better understanding of the specific pathways involved in osteocyte death could eventually lead to the development of novel strategies to modulate the rate of OTM.

CONCLUSIONS

- In an *in vivo* mouse model of OTM, significant osteocyte death occurred on the compression side of the alveolar bone at 12, 24, and 72 hours after loading, before osteoclast recruitment.
- During this initial time, osteocyte caspase-3 activity increases, but not significantly, pointing toward the fact that mechanisms other than apoptosis might be involved in osteocyte death during OTM.

REFERENCES

1. Meikle MC. The tissue, cellular, and molecular regulation of orthodontic tooth movement: 100 years after Carl Sandstedt. *Eur J Orthod*. 2006;28:221–240.
2. Tan SD, Xie R, Klein-Nulend J, et al. Orthodontic force stimulates eNOS and iNOS in rat osteocytes. *J Dental Res*. 2009;88:255–260.

3. Gluhak-Heinrich J, Ye L, Bonewald LF, et al. Mechanical loading stimulates dentin matrix protein 1 (DMP1) expression in osteocytes *in vivo*. *J Bone Miner Res*. 2003;18:807–817.
4. Gluhak-Heinrich J, Pavlin D, Yang W, MacDougall M, Harris SE. MEPE expression in osteocytes during orthodontic tooth movement. *Arch Oral Biol*. 2007;52:684–690.
5. Tanaka K, Matsuo T, Ohta M, et al. Time-lapse microcinematography of osteocytes. *Miner Electrolyte Metab*. 1995;21:189–192.
6. Zhao S, Zhang YK, Harris S, Ahuja SS, Bonewald LF. MLO-Y4 osteocyte-like cells support osteoclast formation and activation. *J Bone Miner Res*. 2002;17:2068–2079.
7. Kogianni G, Mann V, Noble BS. Apoptotic bodies convey activity capable of initiating osteoclastogenesis and localized bone destruction. *J Bone Miner Res*. 2008;23:915–927.
8. Darzynkiewicz Z, Juan G, Li X, Gorczyca W, Murakami T, Traganos F. Cytometry in cell necrobiology: analysis of apoptosis and accidental cell death (necrosis). *Cytometry*. 1997;27:1–20.
9. Bran GM, Stern-Straeter J, Hormann K, Riedel F, Goessler UR. Apoptosis in bone for tissue engineering. *Arch Med Res*. 2008;39:467–482.
10. Porter AG, Janicke RU. Emerging roles of caspase-3 in apoptosis. *Cell Death Differ*. 1999;6:99–104.
11. Hamaya M, Mizoguchi I, Sakakura Y, Yajima T, Abiko Y. Cell death of osteocytes occurs in rat alveolar bone during experimental tooth movement. *Calcif Tissue Int*. 2002;70:117–126.
12. Sakai Y, Balam TA, Kuroda S, et al. CTGF and apoptosis in mouse osteocytes induced by tooth movement. *J Dent Res*. 2009;88:345–350.
13. Olson C, Uribe F, Kalajzic Z, et al. Orthodontic tooth movement causes decreased promoter expression of collagen type 1, bone sialoprotein and alpha-smooth muscle actin in the periodontal ligament. *Orthod Craniofac Res*. 2012;15:52–61.
14. Bellido T. Osteocyte-driven bone remodeling. *Calcif Tissue Int*. 2014;94:25–34.
15. Bonewald LF. The amazing osteocyte. *J Bone Miner Res*. 2011;26:229–238.
16. Cardoso L, Herman BC, Verborgt O, Laudier D, Majeska RJ, Schaffler MB. Osteocyte apoptosis controls activation of intracortical resorption in response to bone fatigue. *J Bone Mineral Res*. 2009;24:597–605.
17. Charriaut-Marlangue C, Ben-Ari Y. A cautionary note on the use of the TUNEL stain to determine apoptosis. *Neuroreport*. 1995;7:61–64.
18. Krysko DV, Vanden Berghe T, Parthoens E, D'Herde K, Vandenabeele P. Methods for distinguishing apoptotic from necrotic cells and measuring their clearance. *Methods Enzymol*. 2008;442:307–341.
19. Broker LE, Kruyt FA, Giaccone G. Cell death independent of caspases: a review. *Clin Cancer Res*. 2005;11:3155–3162.
20. Christofferson DE, Yuan J. Necroptosis as an alternative form of programmed cell death. *Curr Opin Cell Biol*. 2010;22:263–268.
21. Kaczmarek A, Vandenabeele P, Krysko DV. Necroptosis: the release of damage-associated molecular patterns and its physiological relevance. *Immunity*. 2013;38:209–223.
22. Matsumoto T, Imura T, Ogura K, Moriyama K, Yamaguchi A. The role of osteocytes in bone resorption during orthodontic tooth movement. 2013;92:340–345.